

Reverse and Forward Engineering of Local Voltage Control in Distribution Networks

Xinyang Zhou, Lijun Chen, Masoud Farivar, Zhiyuan Liu, and Steven Low

Abstract—The increasing penetration of renewable and distributed energy resources in distribution networks calls for fast and efficient distributed voltage regulation algorithms. In this work we study local Volt/VAR control by first reverse engineering the existing non-incremental control scheme together with a linearized power flow equation as a well-defined convex optimization problem, based on which we characterize the properties of its equilibrium point. We then design two incremental local algorithms for solving the same optimization problem with less restrictive convergence conditions and better voltage regulation through forward engineering. We compare the performance of the three algorithms with both analytical characterization and numerical evaluation.

Index Terms—Distributed control and optimization, voltage regulation, Volt/VAR control, network dynamics as optimization algorithms, power networks, reverse and forward engineering.

I. INTRODUCTION

Capacitor banks and load tap changers are traditionally utilized to control voltage levels across a distribution system [1], [2]. Given the predictable and slow changes in power demand, switching operations were required only a few times per day. However, with the increasing penetration of renewable energy resource like photovoltaic (PV) and wind turbines in both residential and commercial settings [3], [4], the intermittence and fast-changing renewable energy supply introduces rapid fluctuations that are beyond the traditional voltage regulation schemes, and calls for new voltage control paradigms. Even though the current IEEE Standard 1547 [5] requires distributed generation to operate at unity power factor, PV inverters can readily adjust real and reactive power outputs to stabilize voltages and cope with fast time-varying conditions. Indeed the IEEE Standards group is actively exploring a new inverter-based volt/var control. Unlike the capacity banks or ULTC, inverters can push and pull reactive power much faster, in a much finer granularity, and with low operation costs. They will enable real-time distributed Volt/VAR control that is in need for the future power grids.

A. Inverter-Based Voltage Regulation

Inverter-based voltage regulation has been studied extensively in literature. Related works can be found in the following categories:

X. Zhou, L. Chen and Z. Liu are with College of Engineering and Applied Science, University of Colorado, Boulder, CO 80309, USA (Emails: {xinyang.zhou, lijun.chen, zhiyuan.liu}@colorado.edu).

M. Farivar is with Google. (email: mfarivar@gmail.com).

S. Low is with the Division of Engineering and Applied Science, California Institute of Technology, Pasadena, CA 91125, USA (Email: slow@caltech.edu).

Preliminary results of this paper have been presented at IEEE Conference on Decision and Control (CDC), Florence, Italy, 2013 [54], IEEE International Conference on Smart Grid Communication, Miami, FL, 2015 [55], and Annual Allerton Conference on Communication, Control, and Computing, Allerton, IL, 2015 [56].

- 1) Centralized control: By collecting all the required information and computing a global optimal power flow (OPF) problem, a central controller determines optimal set points for the whole network. Centralized control can approach general objectives and operational constraints, but suffers from huge communication and computation costs if the size of the problem is large, and is thus not scalable. For the same reasons, centralized control usually cannot provide fast real-time control. See, e.g., [6]–[10].
- 2) Distributed control: For OPF problems of certain structures, one can design algorithms to distribute the amount of computation with coordinative communication, which is conducted either between a central controller and agents in a hierarchical way, e.g., [11]–[18], or among neighborhood of individual agent without a central controller, e.g., [19]–[24]. Distributed control provides a scalable way to solve a global OPF problem and can therefore provide fast real-time control.
- 3) Local control: Based on only local information and certain control schemes, local control can provide fast response without any communication within or among control hierarchies; see, e.g., [25]–[31].

We also refer to [32] for a recent comprehensive survey of distributed optimization and control algorithms in power systems.

In this work, we focus on analysis and design of local voltage control. Based on local information and control strategies, local voltage control have simple implementation without communication with other control nodes or central coordinators. However, characterization of its performance, especially from a global perspective as well as its dynamic properties, is challenging. In literature, a lot of works, e.g., [31], [33], lack analytical characterization. Works including [29], [30] give stability analysis, but lack a global perspective in terms of its performance. There are also works providing rigorous performance analysis but are subject to special control functions; e.g., [26], [34] focus on linear local control functions without deadband, while [25] studies quadratic control functions.

B. Reverse and Forward Engineering

We seek a principled way to guide systematic design of local voltage controls with global perspective through the approach of reverse and forward engineering. We first develop models to understand the system-wide properties arising from the interaction among local controls, in particular, whether the power system dynamics with the existing controls can be interpreted as distributed algorithms for solving certain optimization problems, i.e., network dynamics as optimization

algorithms. We then design new distributed control schemes according to distributed algorithms for solving the resulting optimization problem.

Specifically, we first lay out a general framework for reverse engineering voltage dynamics with general non-incremental local voltage control functions, to reveal that they together serve as a distributed algorithm for solving a well-defined convex optimization problem by showing the equivalence between the equilibrium conditions of the control dynamics and the optimality conditions of the optimization problem. The optimization-based model not only characterizes the equilibrium of the local voltage control dynamics from a global perspective, but also suggests a principled way to further design algorithms of desired properties. In this work, motivated by the unsatisfying performance of the non-incremental local control in terms of its restrictive convergence condition and the resultant limited voltage regulation outcomes, we first propose an incremental local control based on the (sub)gradient algorithm for solving the same optimization problem with less restricted convergence condition, and then a pseudo-gradient-based incremental local control that demonstrates even better convergence properties and simpler implementation than the (sub)gradient control while achieving the same equilibrium point as the previous ones.

Similar ideas of reverse and forward engineering were first proposed to understand dynamic behaviors of existing network protocols and guide systematic design of better or new ones in communication networks; see, e.g., [35]–[38]. This line of work has led to the development of a promising mathematical theory for communication network architecture and protocol design—layering as optimization decomposition; see, e.g., [39]–[42]. The layering as optimization decomposition framework views various protocol layers as carrying out distributed computation over the network to optimize a global objective function. Different layers iterate on different subsets of decision variables to achieve individual optimality. Taken together, these local algorithms achieve a global objective. We aim to develop a similar framework—network dynamics as optimization algorithm—for distributed real-time control and optimization of power networks. There are, however, fundamental differences between power and communication networks, in particular, the control/operation of power network cannot be decoupled from the physics of electricity while the control/operation of communication network can be decoupled from the physics of information. This requires designing distributed optimization algorithms that exploit or can be implemented as power system dynamics.

Reverse and forward engineering is thence applied to more diverse classes of works. [43], [44] reverse engineer the frequency dynamics with general primary frequency control and frequency response as a distributed algorithm to solve a cost minimization problem for frequency control subject to the power balance and design improve control schemes based on it. [45] shows that the coupled oscillator system when restricted to a proper region is a distributed partial primal-dual gradient algorithm for solving a well-defined convex optimization problem and its dual, and therefore characterizes the synchronization condition of networked coupled oscillators

through a simple problem of verifying synchronization solution of a system of linear equations. [46], [47] characterize the equilibrium resulting from the load balancing and speed scaling interaction in computer and communication systems through reverse engineering, and introduce optimal load-balancing designs. [48] characterizes dynamic network resource allocation algorithms based on the proportional control in general resource allocation problem through reverse engineering and shows that they achieve both fast response and convergence.

The rest of this paper is organized as follows. Section II models the system and introduces local Volt/VAR control. Section III studies the equilibrium and dynamics of non-incremental local control by reverse engineering. Section IV–IV-B propose two incremental local control schemes to improve the non-incremental one. Section V provides numerical examples and Section VI concludes this paper.

II. NETWORK MODEL AND LOCAL VOLTAGE CONTROL

Consider a tree graph $\mathcal{G} = \{\mathcal{N} \cup \{0\}, \mathcal{L}\}$ that represents a radial distribution network consisting of $n+1$ buses and a set \mathcal{L} of undirected lines between these buses. Bus 0 is the substation bus (slack bus) and is assumed to have a fixed voltage of 1 p.u. Let $\mathcal{N} := \{1, \dots, n\}$ with a size of $\#\mathcal{N} = n$ with $\#$ denoting the cardinality of a set. Due to the tree topology, we also have $\#\mathcal{L} = n$. For each bus $i \in \mathcal{N}$, denote by $\mathcal{L}_i \subseteq \mathcal{L}$ the set of lines on the unique path from bus 0 to bus i , p_i^c and p_i^g the real power consumption and generation, and q_i^c and q_i^g the reactive power consumption and generation, respectively. Let v_i be the squared magnitude of the complex voltage (phasor) at bus i . For each line $(i, j) \in \mathcal{L}$, denote by r_{ij} and x_{ij} its resistance and reactance, and P_{ij} and Q_{ij} the real and reactive power from bus i to bus j respectively. Let ℓ_{ij} denote the squared magnitude of the complex branch current (phasor) from bus i to bus j .

A. Linearized Branch Flow Model

We adopt the following branch flow model introduced in [1], [2] (*DistFlow equations*) to model a *radial* distribution system:

$$P_{ij} = p_j^c - p_j^g + \sum_{k:(j,k) \in \mathcal{L}} P_{jk} + r_{ij}\ell_{ij}, \quad (1a)$$

$$Q_{ij} = q_j^c - q_j^g + \sum_{k:(j,k) \in \mathcal{L}} Q_{jk} + x_{ij}\ell_{ij}, \quad (1b)$$

$$v_j = v_i - 2(r_{ij}P_{ij} + x_{ij}Q_{ij}) + (r_{ij}^2 + x_{ij}^2)\ell_{ij}, \quad (1c)$$

$$\ell_{ij}v_i = P_{ij}^2 + Q_{ij}^2. \quad (1d)$$

Following [49] we assume that the terms involving ℓ_{ij} are zero for all $(i, j) \in \mathcal{L}$ in (1). This approximation neglects the higher order real and reactive power loss terms. Since losses are typically much smaller than power flows P_{ij} and Q_{ij} , it only introduces a small relative error, typically on the order of 1%.

With the above approximations the model (1) simplifies to the following linear model:

$$\begin{aligned} P_{ij} &= \sum_{k \in \beta(j)} (p_k^c - p_k^g), \\ Q_{ij} &= \sum_{k \in \beta(j)} (q_k^c - q_k^g), \\ v_i - v_j &= r_{ij} P_{ij} + x_{ij} Q_{ij}, \end{aligned}$$

where $\beta(j)$ is the set of all descendants of bus j including bus j itself, i.e., $\beta(j) = \{i | \mathcal{L}_j \subseteq \mathcal{L}_i\}$. This yields an explicit solution for v_i in terms of v_0 (which is given and fixed):

$$\begin{aligned} v_0 - v_i &= \sum_{(j,k) \in \mathcal{L}_i} 2r_{jk} P_{jk} + \sum_{(j,k) \in \mathcal{L}_i} 2x_{jk} Q_{jk} \\ &= \sum_{(j,k) \in \mathcal{L}_i} 2r_{jk} \left(\sum_{h \in \beta(k)} (p_h^c - p_h^g) \right) + \sum_{(j,k) \in \mathcal{L}_i} 2x_{jk} \left(\sum_{h \in \beta(k)} (q_h^c - q_h^g) \right) \\ &= \sum_{j \in \mathcal{N}} (p_j^c - p_j^g) \left(\sum_{(h,k) \in \mathcal{L}_i \cap \mathcal{L}_j} 2r_{hk} \right) + \sum_{j \in \mathcal{N}} (q_j^c - q_j^g) \left(\sum_{(h,k) \in \mathcal{L}_i \cap \mathcal{L}_j} 2x_{hk} \right) \\ &= \sum_{j \in \mathcal{N}} R_{ij} (p_j^c - p_j^g) + \sum_{j \in \mathcal{N}} X_{ij} (q_j^c - q_j^g), \end{aligned}$$

where

$$R_{ij} := \sum_{(h,k) \in \mathcal{L}_i \cap \mathcal{L}_j} 2 \cdot r_{hk}, \quad X_{ij} := \sum_{(h,k) \in \mathcal{L}_i \cap \mathcal{L}_j} 2 \cdot x_{hk}. \quad (2)$$

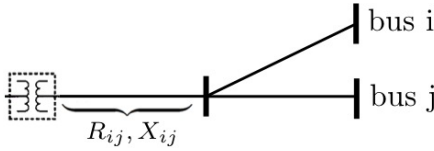


Fig. 1. $\mathcal{L}_i \cap \mathcal{L}_j$ for two arbitrary buses i, j in the network and the corresponding mutual voltage-to-power-injection sensitivity factors R_{ij}, X_{ij} .

Fig. 1 gives an illustration of $\mathcal{L}_i \cap \mathcal{L}_j$ for two arbitrary buses i and j in a radial network and the corresponding R_{ij} and X_{ij} . Since

$$R_{ij} = \frac{dv_i}{dp_j^g} = -\frac{dv_i}{dp_j^c}, \quad (3a)$$

$$X_{ij} = \frac{dv_i}{dq_j^g} = -\frac{dv_i}{dq_j^c}, \quad (3b)$$

R_{ij}, X_{ij} are also referred to as the mutual voltage-to-power-injection sensitivity factors.

Define a resistance matrix $R = [R_{ij}]_{n \times n}$ and a reactance matrix $X = [X_{ij}]_{n \times n}$. Both matrices are positive and symmetric. With the matrices R and X the linearized branch flow model can be summarized compactly as:

$$v = \bar{v}_0 + R(p^g - p^c) + X(q^g - q^c), \quad (4)$$

where $\bar{v}_0 = [v_0, \dots, v_0]^T$ is an n -dimensional vector. In this paper we assume that \bar{v}_0, p^g, p^c, q^c are given constants. The only variables are (column) vectors $v := [v_1, \dots, v_n]^T$ of squared voltage magnitudes and $q^g := [q_1^g, \dots, q_n^g]^T$ of generated reactive powers. Let $\bar{v} = \bar{v}_0 + R(p^g - p^c) - Xq^c$, which is a constant vector. For notational simplicity, in the rest of the

paper we will ignore the superscript in q^g and write q instead. Then the linearized branch flow model reduces to the following simple form:

$$v = Xq + \bar{v}. \quad (5)$$

The following result is important for the rest of this paper.

Lemma 1 *The matrices R and X are positive definite.* \square

Proof: The proof uses the fact that the resistances and reactances values of power lines in the network are all positive. Here we give a proof for the reactance matrix X , and exactly the same argument applies to the resistance matrix R .

We prove by induction on the number k of buses in the network, excluding bus 0 (the root bus). The base case of $k = 1$ corresponds to a two-bus network with one line. Here X is obviously a positive scalar that is equal to the reactance of the line connecting the two buses.

Suppose that the theorem holds for all $k \leq n$. For the case of $k = n + 1$ we consider two possible network topologies as shown in Figure 2:

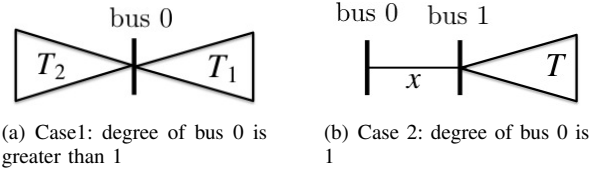


Fig. 2. Two possible network structures

Case 1: bus 0 is of degree greater than 1. Split the network into two different trees rooted at bus 0, denoted by T_1 and T_2 , each of which has no more than n buses excluding bus 0. Denote by X_1 and X_2 respectively the reactance matrices of \mathcal{T}_1 and \mathcal{T}_2 . By induction assumption X_1 and X_2 are positive definite. Note that the set \mathcal{L}_i of lines on the unique path from bus 0 to bus i must completely lie inside either \mathcal{T}_1 or \mathcal{T}_2 , for all i . Therefore, by definition (2), the reactance matrix X of the network has the following block-diagonal form:

$$X_{ij} = \begin{cases} X_{1ij}, & i, j \in \mathcal{T}_1 \\ X_{2ij}, & i, j \in \mathcal{T}_2 \\ 0, & \text{otherwise} \end{cases} \Rightarrow X = \begin{bmatrix} X_1 & 0 \\ 0 & X_2 \end{bmatrix}.$$

Since X_1 and X_2 are positive definite, so is X .

Case 2: bus 0 is of degree 1. Suppose without loss of generality that bus 0 is connected to bus 1. Denote by x the reactance of the line connecting buses 0 and 1, and \mathcal{T} the tree rooted at bus 1, excluding bus 0. Denote by Y the reactance matrix of \mathcal{T} , and by induction assumption, Y is positive definite. Note that, for all buses i in the network, the set \mathcal{L}_i includes the single line that connects buses 0 and 1. Therefore, by definition (2), the reactance matrix X has the following form:

$$X_{ij} = \begin{cases} Y_{ij} + x, & i, j \in \mathcal{T} \\ x, & \text{otherwise} \end{cases} \Rightarrow X = \begin{bmatrix} x & \dots & x \\ \vdots & & \vdots \\ x & \dots & x \end{bmatrix} + \begin{bmatrix} 0 & 0 \\ 0 & Y \end{bmatrix},$$

One can verify that, when Y is positive definite and x is positive, X is positive definite. This concludes the proof. \blacksquare

B. Inverter Model

We consider an inverter at bus i that can generate non-negative real power p_i^g and reactive power q_i^g that can have either sign. p_i^g and q_i^g are constrained by the apparent power capability s_i of the inverter as follows:

$$0 \leq p_i^g \leq s_i, \quad 0 \leq q_i^g \leq s_i, \quad p_i^{g2} + q_i^{g2} \leq s_i^2. \quad (6)$$

Consider power ratio $\cos \rho_i$ with $0 \leq \rho_i \leq \pi/2$ such that

$$p_i^g/s_i^g \geq \cos \rho_i. \quad (7)$$

Given non-controllable $p_i^g \leq s_i$, the feasible power set Ω_i for inverter i is cast as:

$$\Omega_i := \{q_i \mid q_i^{\min} \leq q_i \leq q_i^{\max}\}, \quad (8)$$

where

$$q_i^{\max} = \min \left\{ p_i^g \tan \rho_i, \sqrt{s_i^2 - p_i^{g2}} \right\},$$

$$q_i^{\min} = \max \left\{ -p_i^g \tan \rho_i, -\sqrt{s_i^2 - p_i^{g2}} \right\},$$

based on (6)–(7). Here, p_i^g is further assumed to be sized appropriately to provide enough freedom in q_i [31]. Please also refer to [13] for more general PV inverter modeling.

For buses without inverters, we can set $s_i = p_i^g = q_i^g = 0$ and $\Omega_i = \{0\}$. Define $\Omega := \prod_{i=1}^n \Omega_i$ for notational simplicity.

C. Local Volt/VAR Control

The goal of Volt/VAR control in a distribution network is to maintain the bus voltages v to within a tight range around their nominal values $v_i^{\text{nom}} = 1$ p.u., $i \in \mathcal{N}$ by provisioning reactive power injections $q := (q_1, \dots, q_n)$. Without losing generality, we also assume that v_i^{nom} are identical at all buses. This can be modeled as a feedback dynamical system with state $(v(t), q(t))$ at discrete time t . A general Volt/VAR control algorithm maps the current state $(v(t), q(t))$ to a new reactive power injections $q(t+1)$. The new $q(t+1)$ produces a new voltage magnitudes $v(t+1)$ according to (5). Usually $q(t+1)$ is determined either completely or partly by a certain Volt/VAR control function defined as follows:

Definition 1 A Volt/VAR control function $f : \mathbb{R}^n \rightarrow \mathbb{R}^n$ is a collection of local control functions $f_i : \mathbb{R} \rightarrow \mathbb{R}$, each of which maps the current local voltage v_i to a local control variable $u_i(q_i)$ in reactive power at bus i :

$$u_i(q_i) = f_i(v_i). \quad \forall i \in \mathcal{N}. \quad (9)$$

□

The control functions f_i are designed to be decreasing but not always strictly decreasing because of a potential deadband, where the control signal $u_i(q_i)$ is set to zero to prevent oscillatory behavior. Assume that for each bus $i \in \mathcal{N}$ a symmetric deadband $(-\delta_i/2, \delta_i/2)$ with $\delta_i \geq 0$. Further, the following two assumptions are made for the control functions.

Assumption 1 The Volt/VAR control functions f_i are non-increasing over \mathbb{R} and strictly decreasing and differentiable in

$(-\infty, -\delta_i/2)$ and in $(\delta_i/2, +\infty)$, i.e., there exist $\underline{\alpha}_i > 0$ such that $|f_i'(v_i)| \geq \underline{\alpha}_i$, $\forall v_i \in (-\infty, -\delta_i/2)$ and $\forall v_i \in (\delta_i/2, +\infty)$, $\forall i \in \mathcal{N}$. □

Assumption 2 The derivative of the control function f_i is upper-bounded, i.e., there exist $\bar{\alpha}_i > 0$ such that $|f_i'(v_i)| \leq \bar{\alpha}_i$ for all feasible v_i , $\forall i \in \mathcal{N}$. □

Assumption 1 prevents control functions from being completely flat and thus useless. Assumption 2 guarantees that an infinitesimal change in voltage should not lead to a jump in the control variable. See Fig. 3 (left) for an illustrative example of control function based on a piecewise linear droop control function [5]:

$$f_i(v_i) = -\alpha_i [v_i - \delta_i/2]^+ + \alpha_i [-v_i - \delta_i/2]^+, \quad (10)$$

with slope $\underline{\alpha}_i \leq \alpha_i \leq \bar{\alpha}_i$. Note that our design and analysis for the rest of the paper are not limited to linear control functions.

The Volt/VAR control function (9) together with the linear power flow equation (5) constitutes the following non-incremental local Volt/VAR dynamical system \mathcal{D}_1 :

$$\begin{cases} v(t) = Xq(t) + \tilde{v} \\ q_i(t+1) = [f_i(v_i(t) - v_i^{\text{nom}})]_{\Omega_i}, \end{cases} \quad (11a)$$

$$(11b)$$

where $[\]_{\Omega_i}$ denotes the projection onto the set Ω_i . A fixed point (v^*, q^*) of the above dynamical system, defined as follows, represents an equilibrium operating point of the network.

Definition 2 (v^*, q^*) is called an equilibrium point of \mathcal{D}_1 , if it satisfies

$$v^* = Xq^* + \tilde{v}, \quad (12a)$$

$$q^* = [f(v^* - v^{\text{nom}})]_{\Omega}, \quad (12b)$$

with $\Omega := \prod_{i=1}^n \Omega_i$. □

In next section, we characterize the defined equilibrium point of local Volt/VAR control \mathcal{D}_1 through reverse engineering and study its dynamical properties.

III. REVERSE ENGINEERING: EQUILIBRIUM AND DYNAMICS

A. Reverse Engineering

Since f_i is non-increasing, a (generalized) inverse f_i^{-1} exists. In particular, at the origin, we assign $f_i^{-1}(0) = 0$ in the deadband $[-\delta_i/2, \delta_i/2]$. This may introduce a discontinuity at $q_i = 0$ if the deadband $\delta_i > 0$, with

$$f_i^{-1}(0^+) \leq -\delta_i/2, \text{ and } f_i^{-1}(0^-) \geq \delta_i/2. \quad (13)$$

Define a cost function for provisioning reactive power at each bus $i \in \mathcal{N}$ as:

$$C_i(q_i) := - \int_0^{q_i} f_i^{-1}(q) dq, \quad (14)$$

which is convex since f_i^{-1} is decreasing. See Fig. 3 (middle and right) for an example based on the inverse of piece-wise linear control function (10). Then, given any $v_i(t)$, $q_i(t+1)$

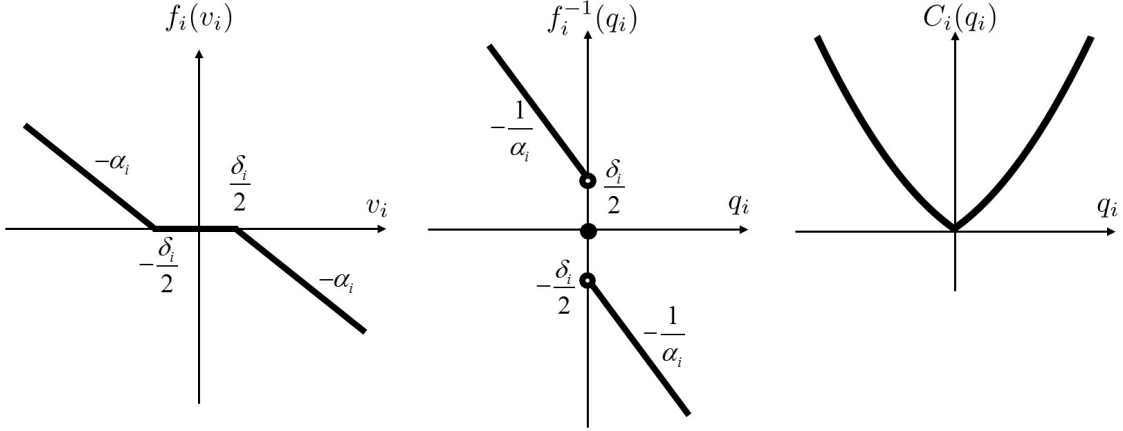


Fig. 3. From left to right: (left) piecewise linear Volt/VAR control curve based on the piecewise linear function (10), (middle) its inverse function, and (right) the corresponding cost function (14), i.e., the integral of inverse function.

in (11b) is the unique solution to the following distributed optimization problem:

$$q_i(t+1) = \arg \min_{q_i \in \Omega_i} C_i(q_i) + q_i (v_i(t) - v_i^{\text{nom}}), \quad (15)$$

i.e., (11b) and (15) are equivalent specification of $q_i(t+1)$.

Consider now the function $F(q) : \Omega \rightarrow \mathbb{R}$:

$$F(q) := C(q) + \frac{1}{2} q^\top X q + q^\top \Delta \tilde{v}, \quad (16)$$

where $C(q) = \sum_{i \in \mathcal{N}} C_i(q_i)$ and $\Delta \tilde{v} := \tilde{v} - v^{\text{nom}}$, and a global optimization problem:

$$\min_{q \in \Omega} F(q). \quad (17)$$

Theorem 1 *Suppose Assumption 1 holds. Then \mathcal{D}_1 has a unique equilibrium point. Moreover, a point (v^*, q^*) is an equilibrium of \mathcal{D}_1 if and only if q^* is the unique optimal solution of (17) and $v^* = Xq^* + \tilde{v}$. \square*

Proof: From Lemma 1 the matrix X is positive definite. This implies that the objective function $F(q)$ is *strictly* convex. Hence, the first-order optimality condition for (17) is both necessary and sufficient; moreover, (17) has a unique optimal solution. We next relate it to the equilibrium point of \mathcal{D}_1 .

The (sub)gradient of F is the following vector:

$$\begin{aligned} \nabla F(q) &= \nabla C(q) + Xq + \Delta \tilde{v} \\ &= \nabla C(q) + (Xq + \tilde{v}) - v^{\text{nom}}, \end{aligned}$$

where, by the definition of $C_i(q_i)$,

$$\nabla C(q) = [-f_1^{-1}(q_1), \dots, -f_n^{-1}(q_n)]^\top.$$

Therefore, the first-order optimality condition for (17) is:

$$q^* = f(Xq^* + \tilde{v} - v^{\text{nom}}).$$

It follows that a point (v^*, q^*) is an equilibrium of \mathcal{D}_1 if and only if q^* solves (17) and $v^* = Xq^* + \tilde{v}$. The existence and uniqueness of the optimal solution of (17) then implies that of the equilibrium (v^*, q^*) . \blacksquare

Further with $v = Xq + \tilde{v}$, the objective can be equivalently cast as:

$$F(q, v) = C(q) + \frac{1}{2} (v - v^{\text{nom}})^\top X^{-1} (v - v^{\text{nom}}) - \frac{1}{2} \Delta \tilde{v}^\top X^{-1} \Delta \tilde{v}. \quad (18)$$

Noticing that the last term is a constant, we conclude that the local Volt/VAR control \mathcal{D}_1 seeks an optimal trade-off between minimizing the cost of reactive power provisioning $C(q)$, and minimizing the cost of voltage deviation $\frac{1}{2} (v - v^{\text{nom}})^\top X^{-1} (v - v^{\text{nom}})$, roughly. We next provide more detailed and accurate characterization of the objective function (18).

B. Equilibrium Characterization: A Closer Look

We characterize the equilibrium of \mathcal{D}_1 through equivalently studying the solution point of (17) based on the form of (18). Specifically, aside from the well-interpreted term $C(q)$ as the cost of reactive power provisioning and the constant term $-\frac{1}{2} \Delta \tilde{v}^\top X^{-1} \Delta \tilde{v}$, we focus on the voltage deviation term $\frac{1}{2} (v - v^{\text{nom}})^\top X^{-1} (v - v^{\text{nom}})$ in this part.

To this end, we first consider the topology where bus 0 is of degree 1, and we will discuss the extension to the topology where bus 0 is of degree greater than 1 later.

1) *Bus 0 is of Degree 1:* We denote \mathcal{T} the subtree rooted at bus 1 **excluding bus 0**. Define the inverse tree \mathcal{T}' of \mathcal{T} that shares the same buses and lines set as \mathcal{T} , but with inverse reactance line weight $1/x_{ij}$. Let $\mathbb{L} \in \mathbb{R}^{n \times n}$ be the weighted Laplacian matrix of \mathcal{T}' defined as follows:

$$\mathbb{L}_{ij} = \begin{cases} -1/x_{ij}, & (i, j) \in \mathcal{L}, i \neq j \\ \sum_{(i,k) \in \mathcal{L}} 1/x_{ik}, & i = j \\ 0, & \text{otherwise} \end{cases}.$$

Recalling that x denotes the reactance of the line connecting buses 0 and 1, we have the following result proposed by Liu, et al. [50].

Theorem 2 (Theorem in [50]) *Given the tree graph $\mathcal{G} = \{\mathcal{N} \cup \{0\}, \mathcal{L}\}$ with bus 0 being of degree 1 and its reactance*

matrix X defined by (2), the inverse matrix X^{-1} has the following explicit form:

$$X^{-1} = \mathbb{L} + \begin{bmatrix} 1/x & 0 & \cdots & 0 \\ 0 & 0 & \cdots & 0 \\ \vdots & \vdots & \ddots & \vdots \\ 0 & 0 & \cdots & 0 \end{bmatrix}. \quad (19)$$

□

Proof: We provide a simplified proof here, and refer to [50] for more detailed discussions. To show that (19) is the inverse of X , it is equivalent to show that $(XX^{-1})_{ii} = 1, \forall i$ and $(XX^{-1})_{ij} = 0, \forall i \neq j$.

Denote by $\mathbb{N}(i) \in \mathcal{N}$ the set of the neighbor nodes of node i , $\mathbb{C}(i) \in \mathcal{N}$ the set of the children nodes of node i and $\mathbb{P}(i) \in \mathcal{N}$ the set of the parent node of node i . Note that $X_{jj} > X_{ii}, \forall j \in \mathbb{C}(i)$ and that $X_{jj} < X_{ii}, \forall j \in \mathbb{C}(i)$. Also note that $X_{ij}^{-1} = -1/|X_{ii} - X_{jj}| = -1/x_{ij}$ when $j \in \mathbb{N}(i)$, and $X_{ij}^{-1} = 0$ when $j \notin \mathbb{N}(i)$ and $j \neq i$.

(1) We first look at $(XX^{-1})_{ii}$. When $i \neq 1$, i.e., $\mathbb{P}(i) \neq \emptyset$, we have

$$\begin{aligned} (XX^{-1})_{ii} &= \sum_k X_{ik} X_{ki}^{-1} \\ &= X_{ii} X_{ii}^{-1} + \sum_{k \in \mathbb{N}(i)} X_{ik} X_{ki}^{-1} \\ &= X_{ii} X_{ii}^{-1} + \sum_{k \in \mathbb{P}(i)} X_{ik} X_{ki}^{-1} + \sum_{k \in \mathbb{C}(i)} X_{ik} X_{ki}^{-1}. \end{aligned} \quad (20)$$

If $k \in \mathbb{C}(i)$, $X_{ik} X_{ki}^{-1} = X_{ik}/(X_{ii} - X_{kk}) = X_{ii}/(X_{ii} - X_{kk})$; if $k \in \mathbb{P}(i)$, $X_{ik} X_{ki}^{-1} = X_{ik}/(X_{kk} - X_{ii}) = X_{kk}/(X_{kk} - X_{ii})$. Also, $X_{ii} X_{ii}^{-1} = X_{ii} \sum_{k \in \mathbb{N}(i)} \frac{1}{|X_{kk} - X_{ii}|}$. Substituting all these into (20), one has:

$$(XX^{-1})_{ii} = \sum_{k \in \mathbb{P}(i)} \frac{X_{ii} - X_{kk}}{|X_{kk} - X_{ii}|} = \sum_{k \in \mathbb{P}(i)} 1 = \#\mathbb{P}(i) = 1,$$

since each node only has one parent node when $i \neq 1$.

When $i = 1$, we have $\mathbb{P}(1) = \emptyset$. In equation (19), we add $1/x$ which is the inverse reactance of line $(0, 1)$ to the weighted Laplacian matrix of \mathcal{T}' . This makes bus 0 a pseudo parent node of bus 1 which leads to

$$(XX^{-1})_{ii} = \sum_{k \in \mathbb{P}(i) \cup \{0\}} \frac{X_{ii} - X_{kk}}{|X_{kk} - X_{ii}|} = \sum_{k \in \mathbb{P}(i) \cup \{0\}} 1 = \#\mathbb{P}(i) = 1.$$

(2) As for $(XX^{-1})_{ij}$ with $i \neq j$, similar methods are applied to obtain:

$$(XX^{-1})_{ij} = \sum_k X_{ik} X_{kj}^{-1} = \sum_{k \in \mathbb{P}(j)} \frac{X_{ij} - X_{ik}}{|X_{kk} - X_{jj}|}.$$

Two subcases are discussed:

- Subcase 1: $X_{ik} = X_{ii}$ or $X_{ik} \leq \min(X_{ii}, X_{kk}), \forall k$. In this case, it is easy to verify that $X_{ij} = X_{ik}$ which leads to $(XX^{-1})_{ij} = 0$.
- Subcase 2: If $k \in \mathbb{P}(j)$, $X_{ij} = X_{kk}$ and $X_{ik} = X_{kk}$; if $k \in \mathbb{C}(j)$, there exists one special k such that $X_{ik} = X_{kk}$ and for all the other k , $X_{ik} = X_{jj}$. In this case, we can derive

that

$$\begin{aligned} (XX^{-1})_{ij} &= \sum_{k \in \mathbb{P}(j)} \frac{X_{ij} - X_{ik}}{|X_{kk} - X_{jj}|} + \sum_{k \in \mathbb{C}(j)} \frac{X_{ij} - X_{ik}}{|X_{kk} - X_{jj}|} \\ &= \underbrace{1}_{k \in \mathbb{P}(j)} + \underbrace{(-1)}_{\text{special } k \in \mathbb{C}(j)} + \underbrace{+0 + \cdots + 0}_{\text{other } k} \\ &= 0. \end{aligned}$$

This completes the proof. ■

Based on Theorem 2, we are able to recast the cost function (18) as

$$\begin{aligned} F(q, v) &= C(q) + \frac{1}{2} \left(\frac{(v_1 - v_1^{\text{nom}})^2}{x} + \sum_{(i,j) \in \mathcal{L}} \frac{(v_i - v_j)^2}{x_{ij}} \right) \\ &\quad - \frac{1}{2} \Delta \bar{v}^\top X^{-1} \Delta \bar{v}. \end{aligned} \quad (21)$$

Seen from (21), the term for the cost of voltage deviation $(v_1 - v_1^{\text{nom}})^2/x + \sum_{(i,j) \in \mathcal{L}} (v_i - v_j)^2/x_{ij}$ consists of two parts, the first interpreted as the voltage deviation of bus 1 from the nominal value, and the second being the cost of voltage non-consensus of all buses within their neighborhood. Minimizing the two parts together can be seen as an effort to push voltages of all buses towards nominal value while keeping the voltage values of all buses close to each other.

2) *Bus 0 is of Degree $d \geq 1$:* Similar to Lemma 1, we split the tree into d subtrees and write its reactance matrix as

$$X = \begin{bmatrix} X_1 & 0 & \cdots & 0 \\ 0 & X_2 & \cdots & 0 \\ \vdots & \vdots & \ddots & \vdots \\ 0 & 0 & \cdots & X_d \end{bmatrix},$$

where block matrices X_1, \dots, X_d defined by (2) are the reactance matrices for the subtrees. Then Theorem 2 naturally applies to $X_i, \forall i = 1, \dots, d$.

Let x_i denote the reactance of the line connecting buses 0 and subtree i , and \mathbb{L}_i be the weighted Laplacian matrix of (the inverse tree of) subtree i excluding bus 0. Then we have the following result without further proof for the topology where bus 0 has a degree $d \geq 1$.

Corollary 1 *Given the tree graph $\mathcal{G} = \{\mathcal{N} \cup \{0\}, \mathcal{L}\}$ with bus 0 of degree $d \geq 1$, the inverse X^{-1} has the following explicit form:*

$$X^{-1} = \begin{bmatrix} X_1^{-1} & 0 & \cdots & 0 \\ 0 & X_2^{-1} & \cdots & 0 \\ \vdots & \vdots & \ddots & \vdots \\ 0 & 0 & \cdots & X_d^{-1} \end{bmatrix},$$

where the inverse reactance matrix X_i^{-1} for subtree i is calculated as

$$X_i^{-1} = \mathbb{L}_i + \begin{bmatrix} 1/x_i & 0 & \cdots & 0 \\ 0 & 0 & \cdots & 0 \\ \vdots & \vdots & \ddots & \vdots \\ 0 & 0 & \cdots & 0 \end{bmatrix}.$$

□

Based on Corollary 1, the cost function (18) can be expanded similar to (21), with the second term on the right-hand side of (21) extended for subtrees. We omit further details here.

C. Dynamics

We study the dynamic properties of \mathcal{D}_1 with the following convergence condition.

Theorem 3 *Suppose Assumption 1–2 hold. If for all $i \in \mathcal{N}$*

$$\bar{\alpha}_i \sum_j X_{ij} < 1, \quad (22)$$

then the local Volt/VAR control \mathcal{D}_1 converges to the unique equilibrium point (v^, q^*) . Moreover, it converges exponentially fast to the equilibrium. \square*

Proof: Consider a mapping g_1 that is equivalent to \mathcal{D}_1 :

$$q(t+1) = g(q(t)) := f(Xq(t) + \Delta\tilde{v}),$$

whose Jacobian's is calculated as

$$\nabla_q g = \text{diag}(f'_i(v_i - v_i^{\text{nom}}))X.$$

Condition (22) together with Assumption 2 suggests

$$\|\nabla_q g\|_\infty < 1,$$

where the induced matrix norm $\|\cdot\|_\infty$ is the maximum row sum. Hence, for any feasible $q, q' \in \Omega$, one has:

$$\|g(q) - g(q')\|_\infty \leq \|\nabla_q g\|_\infty \cdot \|q - q'\|_\infty < \|q - q'\|_\infty,$$

i.e., mapping g is a contraction, implying that $(v(t), q(t))$ converges exponentially fast to the unique equilibrium point under \mathcal{D}_1 . \blacksquare

D. Discussion and Motivation for Forward Engineering

As discussed, \mathcal{D}_1 seeks an optimal trade-off between minimizing the cost of reactive power provisioning $C(q)$ and minimizing the cost of voltage deviation $\frac{1}{2}(v - v^{\text{nom}})^\top X^{-1}(v - v^{\text{nom}})$. Meanwhile, since $C(q)$ is constructed as the integral of the inverse of control function, the larger the slope α_i is, the smaller the weight of $C(q)$ will be, leading to smaller voltage deviation from nominal value eventually. We use linear control function (10) for illustrative purpose.

We write the inverse of linear control function (10) as

$$f_i^{-1}(q_i) := \begin{cases} -\frac{q_i}{\alpha_i} + \frac{\delta_i}{2}, & \text{if } q_i < 0 \\ 0, & \text{if } q_i = 0 \\ -\frac{q_i}{\alpha_i} - \frac{\delta_i}{2}, & \text{if } q_i > 0 \end{cases}. \quad (23)$$

Then the corresponding cost function for individual reactive power provisioning $C_i(q_i)$ is

$$C_i(q_i) = \begin{cases} \frac{1}{2\alpha_i}q_i^2 - \frac{\delta_i}{2}q_i, & \text{if } q_i \leq 0 \\ \frac{1}{2\alpha_i}q_i^2 + \frac{\delta_i}{2}q_i, & \text{if } q_i > 0 \end{cases}. \quad (24)$$

We refer to Fig. 3 for illustration of $f_i^{-1}(q_i)$ and $C_i(q_i)$ in (23)–(24). As the slope α_i becomes large, the cost of reactive power provisioning $C_i(q_i)$ becomes less weighted compared with the unchanged cost of voltage deviation $\frac{1}{2}(v - v^{\text{nom}})^\top X^{-1}(v - v^{\text{nom}})$. Therefore, given sufficient reactive power supply, better voltage regulation, i.e., smaller voltage deviation from nominal values, can be achieved by applying control functions with steeper slopes. We provide numerical examples in Section V to show this result on a given network (Fig. 5).

On the other hand however, the convergence condition (22) prevents the *non-incremental* control dynamics \mathcal{D}_1 from applying control functions of steep slopes, and therefore limits its voltage regulation performance. This motivates us to design new *incremental* algorithms that break free from the restrictive convergence condition (22) to achieve desired voltage regulation results through forward engineering next.

IV. FORWARD ENGINEERING: IMPROVING VOLTAGE REGULATION AND CONVERGENCE

The optimization-based model (17) not only provides a way to characterize the equilibrium of the local Volt/VAR control, as shown in Theorems 1, but also suggests a principled way to engineer the control. New design goals such as fairness and economic efficiency can be taken incorporated by engineering the objective function in (17), and more importantly, new control schemes with better dynamical properties can be designed based on various optimization algorithms, e.g., the (sub)gradient algorithm.

A. (Sub)gradient Algorithm

We first consider a (sub)gradient method to solve the problem (17). To this end, consider the following local control strategy:

$$q_i(t+1) = \left[q_i(t) - \gamma_2 \frac{\partial F(q(t))}{\partial q_i} \right]_{\Omega_i},$$

where $\gamma_2 > 0$ is the constant stepsize, and the (sub)gradient is calculated as follows:

$$\frac{\partial F(q(t))}{\partial q_i} = \begin{cases} C'_i(q_i(t)) + v_i(t) - v_i^{\text{nom}}, & \text{if } q_i(t) \neq 0 \\ v_i(t) - v_i^{\text{nom}}, & \text{if } q_i(t) = 0, \text{ and} \\ & -\delta/2 \leq v_i(t) - v_i^{\text{nom}} \leq \delta/2 \\ -\delta/2 + v_i(t) - v_i^{\text{nom}}, & \text{if } q_i(t) = 0, \text{ and} \\ & v_i(t) - v_i^{\text{nom}} > \delta/2 \\ \delta/2 + v_i(t) - v_i^{\text{nom}}, & \text{if } q_i(t) = 0, \text{ and} \\ & v_i(t) - v_i^{\text{nom}} < -\delta/2 \end{cases}. \quad (25)$$

The above control algorithm is *incremental* as at each time the reactive power is “gradually” adjusted upon the provisioning at the previous time. It is also distributed, since the reactive power provisioning decision at each bus $i \in \mathcal{N}$ depends only on the current provisioning and voltage at bus i .

We thus obtain the following incremental local Volt/VAR dynamical system \mathcal{D}_2 :

$$v(t) = Xq(t) + \tilde{v} \quad (26a)$$

$$\left\{ \begin{array}{l} q_i(t+1) = \left[q_i(t) - \gamma_2 \frac{\partial F(q(t))}{\partial q_i} \right]_{\Omega_i} \end{array} \right. \quad (26b)$$

The following result is immediate.

Theorem 4 *Suppose Assumption 1 holds. Then there exists a unique equilibrium point for the dynamical system \mathcal{D}_2 . Moreover, a point (v^*, q^*) is an equilibrium if and only if q^* is the unique optimal solution of problem (17) and $v^* = Xq^* + \tilde{v}$. \square*

Denote $\bar{A} := \text{diag}\{\bar{\alpha}_1, \dots, \bar{\alpha}_n\} \in \mathbb{R}_{++}^{N \times N}$, $\bar{A}^{-1} := \text{diag}\{1/\bar{\alpha}_1, \dots, 1/\bar{\alpha}_n\} \in \mathbb{R}_{++}^{N \times N}$, and $\xi_i := \sum_{j \in \mathcal{N}} X_{ij}$. We next

study the dynamical properties of \mathcal{D}_2 , launching with the following two lemmas.

Lemma 2 (Strong convexity) *The objective function (16) is strongly convex, i.e.,*

$$(\nabla_q F(q) - \nabla_q F(q'))(q - q')^\top \geq m\|q - q'\|_2^2, \forall q, q' \in \Omega, \quad (27)$$

where $m \geq \lambda_{\min}(\bar{A}^{-1} + X) > 0$. \square

Lemma 2 is immediate because of the positive definite X and \bar{A}^{-1} .

Lemma 3 *Given $\epsilon > 0$, for $\forall q, q' \in \Omega$ with $\|q - q'\|_2 \geq \epsilon$, we have*

$$\|\nabla F(q) - \nabla F(q')\|_2 \leq L(\epsilon)\|q - q'\|_2, \quad (28)$$

where $L(\epsilon)$ satisfies

$$\sum_{i \in N} (\delta_i/\epsilon) + \sum_{i \in N} (1/\underline{\alpha}_i) + \max_{i \in N} (\xi_i) < L(\epsilon) < \infty. \quad (29)$$

\square

Proof: Due to the non-differentiability of $F(q)$ at 0, we prove the lemma by discussing the three following cases:

(i) $q > 0$ & $q' > 0$, or $q < 0$ & $q' < 0$: Lipschitz continuity holds for ∇F . Therefore, for $\forall L(\epsilon) > \max_{i \in N} (\xi_i + 1/\underline{\alpha}_i)$, (28) holds regardless of ϵ .

(ii) $q > 0$ & $q' < 0$, or $q < 0$ & $q' > 0$: ∇F is not continuous at zero. Specifically,

$$\begin{aligned} & \|\nabla F(q) - \nabla F(q')\|_2 \\ &= \|\nabla C(q) - \nabla C(q') + v(q) - v(q')\|_2 \\ &\leq \|f^{-1}(q) - f^{-1}(q')\|_2 + \|v(q) - v(q')\|_2 \\ &\leq \sum_{i \in N} (\delta_i + \|q - q'\|_2/\underline{\alpha}_i) + \max_i \xi_i \cdot \|q - q'\|_2. \end{aligned}$$

Therefore, when (29) holds, (28) follows.

(iii) The rest: all other situations falls between the results of case (i) and (ii). \blacksquare

We now analyze the convergence of \mathcal{D}_2 .

Theorem 5 *Suppose Assumption 1 holds. Given any accuracy $e > 0$, there exists small enough stepsize γ_2 satisfying*

$$\gamma_2 < \frac{2m\epsilon}{L(\epsilon)^2} \quad (30)$$

with $L(\epsilon)$ under (29) and

$$\epsilon + 2m\epsilon^2/L(\epsilon) < e, \quad (31)$$

such that \mathcal{D}_2 converges to the neighborhood of q^* with radius of e . \square

Proof: Consider some constant ϵ such that $0 < \epsilon < e$. When $\|q(t) - q^*\|_2 \geq \epsilon$, we have:

$$\begin{aligned} & \|q(t+1) - q^*\|_2^2 \\ &\leq \|q(t) - \gamma_2 \nabla_q F(q(t)) - q^* + \gamma_2 \nabla_q F(q^*)\|_2^2 \\ &= \|q(t) - q^*\|_2^2 + \gamma_2^2 \|\nabla_q F(q(t)) - \nabla_q F(q^*)\|_2^2 \\ &\quad - 2\gamma_2(q(t) - q^*)^\top (\nabla_q F(q(t)) - \nabla_q F(q^*)) \\ &\leq \|q(t) - q^*\|_2^2 + (\gamma_2^2 L(\epsilon)^2 - 2\gamma_2 m)\|q(t) - q^*\|_2^2, \end{aligned}$$

where the first inequality comes from the non-expansiveness of the projection operator, and the second is due to Lemma 2 and 3. When γ_2 is chosen such that

$$\gamma_2 < \frac{2m}{L(\epsilon)^2}, \quad (32)$$

one has

$$\|q(t+1) - q^*\|_2^2 \leq \|q(t) - q^*\|_2^2,$$

with equality obtained if and only if $q(t) = q^*$, i.e., $\{\|q(t) - q^*\|_2^2\}_t$ is a decreasing sequence when $\|q(t) - q^*\|_2 \geq \epsilon$, and will enter the ball defined as $\|q(t) - q^*\|_2 < \epsilon$ at least once.

Once it enters $\|q(t) - q^*\|_2 < \epsilon$, it will be within the neighborhood of q^* with the bounded radius of

$$\begin{aligned} & \epsilon + \gamma_2 L(\epsilon)\|q - q'\|_2 < \epsilon + \frac{2m\epsilon}{L(\epsilon)} \\ & < \epsilon + \frac{2m\epsilon}{\sum_{i \in N} \delta_i/\epsilon + \sum_{i \in N} 1/\underline{\alpha}_i + \max_i (\xi_i)}. \end{aligned} \quad (33)$$

Because the right-hand side of (33) is monotone in ϵ , approaching to zero when $\epsilon \rightarrow 0$, we can always find small enough ϵ such that $\epsilon + \frac{2m\epsilon}{\sum_{i \in N} \delta_i/\epsilon + \sum_{i \in N} 1/\underline{\alpha}_i + \max_i (\xi_i)} < e$. Therefore, given any accuracy $e > 0$, if we first choose ϵ by (31), and then choose γ_2 by (32), then \mathcal{D}_2 converges to within a ball centered at q^* with a radius of e . \blacksquare

Notice that for any control functions f_i (that satisfies Assumption 1–2), the convergence condition (30) can always be satisfied by a properly chosen stepsize γ_2 for required accuracy e . Even though the range of γ_2 depends on the control functions and the required accuracy, the condition (30) does not constrain the allowable control functions. In contrast, the convergence condition (22) for the non-incremental voltage control \mathcal{D}_1 does constrain the allowable control functions f_i .

However, the (sub)gradient nature of \mathcal{D}_2 may prevent it from converging to the exact optimal point, as indicated by Theorem 5. This could take place when the optimal is close to the non-differentiable point — $q^* = 0$ in this case. Moreover, the (sub)gradient-based control \mathcal{D}_2 incurs implementation complexity, since the (sub)gradient computation (25) requires tracking the value of v_i with respect to deadband $\pm\delta_i/2$, and takes different forms accordingly. Furthermore, it requires the computation of the inverse of the control function f_i , which can be computationally expensive for general control functions. These limitations motivate us to design the next incremental algorithm with better convergence properties and simpler implementation.

B. Pseudo-gradient Algorithm

The pseudo-gradient can provide a good search direction for a problem without requiring the objective function to be differentiable [51]. Consider the following incremental local voltage control strategy based on the pseudo-gradient algorithm for solving the optimization problem (17):

$$q_i(t+1) = [(1 - \gamma_3)q_i(t) + \gamma_3 f_i(v_i(t) - v_i^{\text{nom}})]_{\Omega_i}, \quad (34a)$$

$$= [q_i(t) - \gamma_3(q_i(t) - f_i(v_i(t) - v_i^{\text{nom}}))]_{\Omega_i}, \quad (34b)$$

where $\gamma_3 > 0$ is the constant stepsize/weight. Next we use the presentation of (34a) and (34b) interchangeably.

We obtain the following dynamical system \mathcal{D}_3 with (34):

$$\begin{cases} v(t) = Xq(t) + \tilde{v} & (35a) \\ q_i(t+1) = \left[q_i(t) - \gamma_3(q_i(t) - f_i(v_i(t) - v_i^{\text{nom}})) \right]_{\Omega_i}. & (35b) \end{cases}$$

One can check that the dynamical system \mathcal{D}_3 has the same equilibrium condition as the dynamical systems \mathcal{D}_1 and \mathcal{D}_2 . The following result is immediate.

Theorem 6 *Suppose Assumption 1 holds. There exists a unique equilibrium point for the dynamical system \mathcal{D}_3 . Moreover, a point (v^*, q^*) is an equilibrium if and only if q^* is the unique optimal solution of problem (17) and $v^* = Xq^* + \tilde{v}$. \square*

Given control functions f_i 's, the implementation of the algorithm (34b) is much simpler than \mathcal{D}_2 . We now analyze the convergence of the dynamical system \mathcal{D}_3 . Let $M = \lambda_{\max}(\bar{A}X) > 0$, and we have the following two lemmas.

Lemma 4 (Lipschiz continuity) *Suppose Assumption 1–2 hold. For any $q, q' \in \Omega$, we have*

$$\|f(v(q) - v^{\text{nom}}) - f(v(q') - v^{\text{nom}})\|_2 \leq M\|q - q'\|_2. \quad (36)$$

\square

Lemma 5 *Suppose Assumption 1–2 hold. For any $q, q' \in \Omega$, we have*

$$-M\|q - q'\|_2^2 \leq (q - q')^\top (f(v(q) - v^{\text{nom}}) - f(v(q') - v^{\text{nom}})) \leq 0. \quad (37)$$

\square

Proof: Given positive matrix X , the left-hand side inequality is due to the bounded derivative of f in Assumption 1, while the right-hand side is based on the (not strict) monotonicity of f in Assumption 2. \blacksquare

Theorem 7 *Suppose Assumption 1–2 hold. If the stepsize γ_3 satisfies the following condition:*

$$\gamma_3 \begin{cases} < \frac{2}{1+M^2}, & \text{when } M \geq 1 \\ < \frac{2}{1+M}, & \text{when } 0 < M < 1 \end{cases}, \quad (38)$$

then the dynamical system \mathcal{D}_3 converges to its unique equilibrium point. \square

Proof: We characterize the distance between $q(t+1)$ and the optimal q^* as

$$\begin{aligned} & \|q(t+1) - q^*\|_2^2 \\ & \leq \left\| (1 - \gamma_3)(q(t) - q^*) + \gamma_3(f(v(t) - v^{\text{nom}}) - f(v^* - v^{\text{nom}})) \right\|_2^2 \\ & = (1 - \gamma_3)^2 \|q(t) - q^*\|_2^2 + \gamma_3^2 \|f(v(t) - v^{\text{nom}}) - f(v^* - v^{\text{nom}})\|_2^2 \\ & \quad + 2\gamma_3(1 - \gamma_3)(q(t) - q^*)^\top (f(v(t) - v^{\text{nom}}) - f(v^* - v^{\text{nom}})) \\ & \leq (1 - \gamma_3)^2 \|q(t) - q^*\|_2^2 + \gamma_3^2 M^2 \|q(t) - q^*\|_2^2 \\ & \quad + 2\gamma_3(1 - \gamma_3)(q(t) - q^*)^\top (f(v(t) - v^{\text{nom}}) - f(v^* - v^{\text{nom}})). \end{aligned} \quad (39)$$

We discuss the three following cases.

(i) $0 < \gamma_3 < 1$: By utilizing the right-hand side of (37), (39) follows as

$$\|q(t+1) - q^*\|_2^2 \leq \|q(t) - q^*\|_2^2 + (\gamma_3^2 - 2\gamma_3 + \gamma_3^2 M^2) \|q(t) - q^*\|_2^2.$$

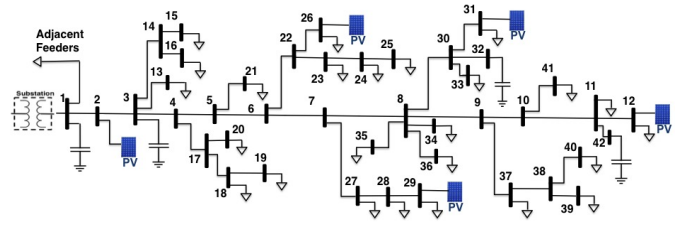


Fig. 4. Circuit diagram for SCE distribution system.

When $\gamma_3 < 2/(1 + M^2)$, $\|q(t+1) - q^*\|_2^2 \leq \|q(t) - q^*\|_2^2$ with equality achieved only if $q(t) = q^*$. Therefore, by Lyapunov stability theorem, \mathcal{D}_3 converges to q^* asymptotically [52].

(ii) $\gamma_3 = 1$: This is when \mathcal{D}_3 is equivalent to \mathcal{D}_1 . The convergence result follows Theorem 3.

(iii) $\gamma_3 > 1$: By utilizing the left-hand side of (37), (39) follows as

$$\begin{aligned} & \|q(t+1) - q^*\|_2^2 \\ & \leq (1 - \gamma_3)^2 \|q(t) - q^*\|_2^2 + \gamma_3^2 M^2 \|q(t) - q^*\|_2^2 \\ & \quad - 2\gamma_3(1 - \gamma_3)M \|q(t) - q^*\|_2^2 \\ & = \|q(t) - q^*\|_2^2 + \gamma_3(M + 1)((M + 1)\gamma_3 - 2) \|q(t) - q^*\|_2^2. \end{aligned}$$

When $\gamma_3 < 2/(1 + M)$, $\|q(t+1) - q^*\|_2^2 \leq \|q(t) - q^*\|_2^2$ with equality holds only if $q(t) = q^*$. Then similar to the argument in case (iii), \mathcal{D}_3 converges to q^* asymptotically.

Conditions in situations (i)–(iii) can be equivalently written in the form of (38). \blacksquare

Theorem 7 guarantees that there always exists small enough stepsize γ_3 such that \mathcal{D}_3 converges to its unique equilibrium point, instead of a region with required accuracy guaranteed for \mathcal{D}_2 .

Remark 1 *Notice that $\gamma_3 \leq 1$ in \mathcal{D}_3 gives a decent interpretation of the new decision $q_i(t+1)$ being a (positively-)weighted sum of the decision $q_i(t)$ at the previous time and the local control $u_i(t) = f_i(v_i(t) - v_i^{\text{nom}})$ in reactive power. However, here we do not require $\gamma_3 \leq 1$ for \mathcal{D}_3 to converge, as long as condition (38) is satisfied.* \square

V. NUMERICAL EXAMPLES

A. Numerical Setup

Consider a modified version of the IEEE 42-bus feeder [5] with zero impedance lines removed and location and capacity of PV generators changed for demonstrated purpose. As shown in Fig. 4, bus 1 is the substation (root bus) and five PV generators are integrated at buses 2, 12, 26, 29, and 31. As we aim to study the Volt/VAR control through PV inverters, all shunt capacitors are assumed to be off. Table I in Appendix contains the network data including the line impedance, the peak MVA demand of loads, and the capacity of the PV generators. It is important to note that all studies are run with a full AC power flow model with MATPOWER [53].

We implement homogeneous piecewise linear droop control functions (10) of the IEEE 1547.8 Standard [5] for all PV inverters, with their deadbands ranging from 0.98 p.u. to 1.02 p.u. and slopes α_i to be determined.

Network Data																	
Line Data				Line Data				Line Data				Load Data		Load Data		PV Generators	
From Bus.	To Bus.	R (Ω)	X (Ω)	From Bus.	To Bus.	R (Ω)	X (Ω)	From Bus.	To Bus.	R (Ω)	X (Ω)	Bus No.	Peak MVA	Bus No.	Peak MVA	Bus No.	Capacity MW
1	2	0.259	0.808	8	34	0.244	0.046	18	19	0.198	0.046	11	0.67	28	0.27		
2	3	0.031	0.092	8	36	0.107	0.031	22	26	0.046	0.015	12	0.45	29	0.2	2	1
3	4	0.046	0.092	8	30	0.076	0.015	22	23	0.107	0.031	13	0.89	31	0.27	26	2
3	13	0.092	0.031	8	9	0.031	0.031	23	24	0.107	0.031	15	0.07	33	0.45	29	1.8
3	14	0.214	0.046	9	10	0.015	0.015	24	25	0.061	0.015	16	0.67	34	1.34	31	2.5
4	17	0.336	0.061	9	37	0.153	0.046	27	28	0.046	0.015	18	0.45	35	0.13	12	3
4	5	0.107	0.183	10	11	0.107	0.076	28	29	0.031	0	19	1.23	36	0.67		
5	21	0.061	0.015	10	41	0.229	0.122	30	31	0.076	0.015	20	0.45	37	0.13		
5	6	0.015	0.031	11	42	0.031	0.015	30	32	0.076	0.046	21	0.2	39	0.45		
6	22	0.168	0.061	11	12	0.076	0.046	30	33	0.107	0.015	23	0.13	40	0.2		
6	7	0.031	0.046	14	16	0.046	0.015	37	38	0.061	0.015	24	0.13	41	0.45		
7	27	0.076	0.015	14	15	0.107	0.015	38	39	0.061	0.015	25	0.2	$V_{base} = 12.35$ KV $S_{base} = 1000$ KVA $Z_{base} = 152.52$ Ω			
7	8	0.015	0.015	17	18	0.122	0.092	38	40	0.061	0.015	26	0.07				
8	35	0.046	0.015	17	20	0.214	0.046					27	0.13				

TABLE I

NETWORK OF FIG. 4: LINE IMPEDANCES, PEAK SPOT LOAD KVA, CAPACITORS AND PV GENERATION'S NAMEPLATE RATINGS.

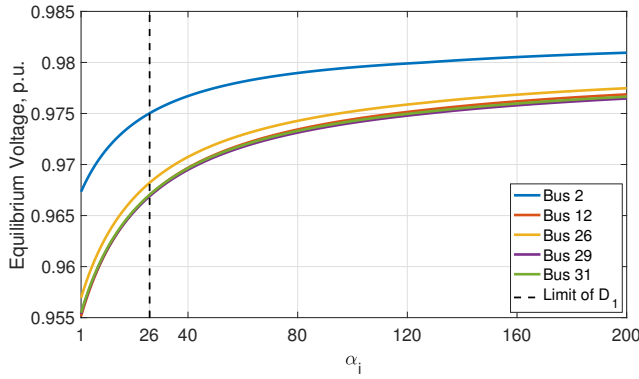


Fig. 5. As the size of α_i increases, better voltage regulation is achieved: the equilibrium voltages v_i^* deviate less from the nominal value.

B. Equilibrium

As discussed in Section III-D, steeper slopes in control functions potentially bring about better voltage regulation. To verify this, we tune α_i from 1 to 200 and record the corresponding equilibrium voltages v^* . As shown in Fig. 5, v^* get closer to v^{nom} as α_i increases. The results confirm our previous discussions that aggressive control functions are to be implemented to pursue less voltage deviation from the nominal value.

C. Dynamics

We examine convergence of dynamics studied in this paper.

1) *Convergence of \mathcal{D}_1* : We increase the value of α_i and observe the dynamics \mathcal{D}_1 . As plotted in Fig. 6, \mathcal{D}_1 displays less stable behaviors as the control functions become more aggressive with the increase of α_i , until it ends up with oscillation when α_i reaches and goes beyond 27. Therefore, under this particular setup, it is impossible for \mathcal{D}_1 to achieve voltage regulation beyond the dash line marked on Fig. 5 due to its divergence.

2) *Convergence of \mathcal{D}_2 and \mathcal{D}_3* : We keep the value of α_i at 27, and implement incremental dynamics. As shown in Fig. 7,

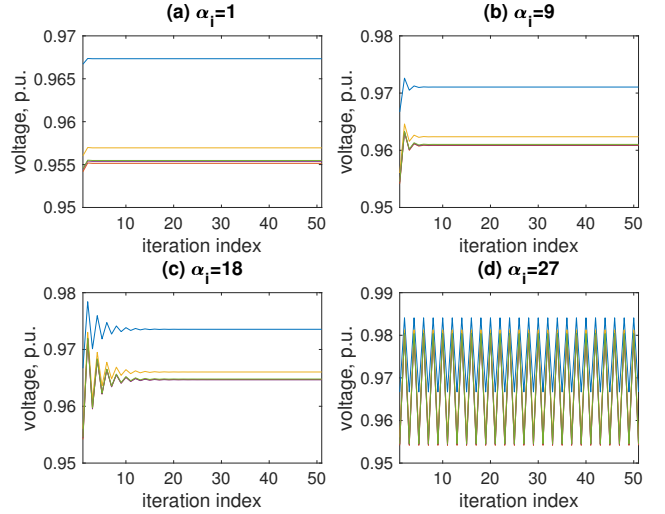


Fig. 6. \mathcal{D}_1 does not converge when the slopes of the control functions become steep ($\alpha_i > 26$ in this case).

while \mathcal{D}_2 and \mathcal{D}_3 do not converge with large stepsizes, one can tune down the value of γ_2 and γ_3 to achieve convergence. This process can always be done with even larger α_i : in fact, the equilibrium points for large α_i in Fig. 5 are all obtained by \mathcal{D}_3 .

3) *Convergence at Non-differentiable Point*: We tune the network configuration such that the optimal reactive power provisioning at certain bus—bus 2 in this case—is close to zero. We compare the performance of \mathcal{D}_2 and \mathcal{D}_3 . As shown in Fig. 8, subgradient algorithm \mathcal{D}_2 eventually converges to a small region around the optimal point, even with very small stepsize and large iteration number. On the other hand, pseudo-gradient algorithm \mathcal{D}_3 converges perfectly to optimal point despite the non-differentiability issue, as shown in Fig. 9. We also zoom into the figures and plot the convergence details in the embedded windows for better illustration.

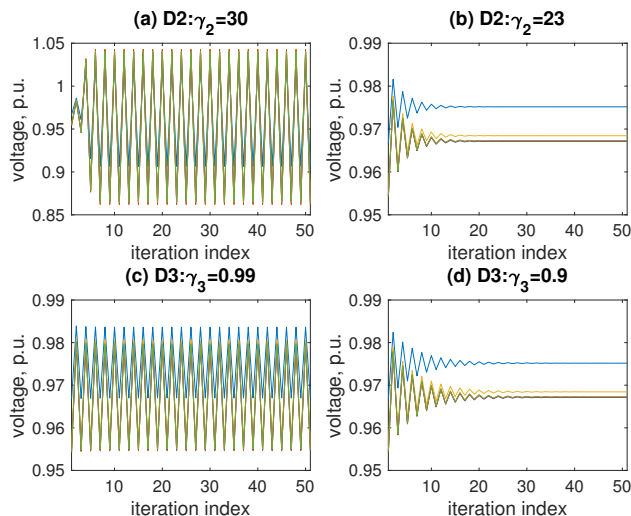


Fig. 7. When $\alpha_i = 27$, \mathcal{D}_1 does not converge (see Fig. 6), while \mathcal{D}_2 and \mathcal{D}_3 converge with small enough stepsizes.

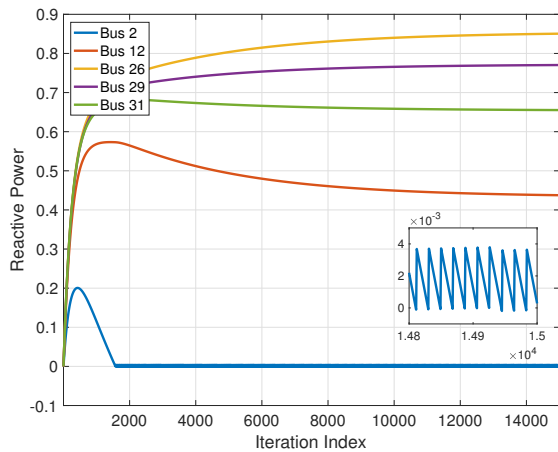


Fig. 8. When the equilibrium point is around non-differentiable point 0, \mathcal{D}_2 converges to a range around the optimality. We zoom in and plot the values of q_2 in the smaller window.

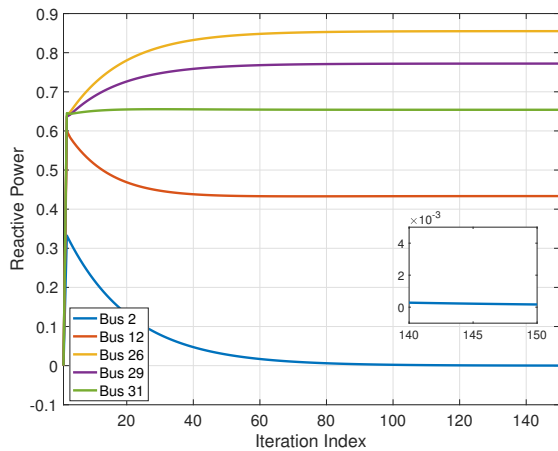


Fig. 9. When the equilibrium point is around non-differentiable point 0, \mathcal{D}_3 converges to the optimal point nevertheless. We zoom in and plot the values of q_2 in the smaller window.

VI. CONCLUSION

We in this paper study local Volt/VAR control with a class of general control functions in distribution networks. We first reverse engineer the existing non-incremental control scheme together with a linearized power flow equation as a well-defined convex optimization problem. By characterizing the optimal point of the optimization problem, we equivalently and thoroughly characterize the equilibrium point of the non-incremental voltage control dynamics. We then propose two incremental control schemes that achieve the same equilibrium point as the non-incremental one but have less restrictive convergence conditions and better voltage regulation. Numerical examples are provided to support the analytical results.

REFERENCES

- [1] M. E. Baran and F. F. Wu, "Optimal capacitor placement on radial distribution systems," *IEEE Trans. on Power Delivery*, vol. 4, no. 1, pp. 725–734, 1989.
- [2] —, "Optimal sizing of capacitors placed on a radial distribution system," *IEEE Trans. on Power Delivery*, vol. 4, no. 1, pp. 735–743, 1989.
- [3] A. McCrone, U. Moslener, F. d'Estais, and C. Grüning, "Global trends in renewable energy investment," 2017.
- [4] REN21, "Renewables 2017 global status report," 2017.
- [5] Standards Coordinating Committee 21 of Institute of Electrical and Electronics Engineers, Inc., IEEE Standard, P1547.8TM/D8, "Recommended practice for establishing methods and procedures that provide supplemental support for implementation strategies for expanded use of IEEE Standard 1547," *IEEE ballot document*, Aug. 2014.
- [6] V. Kekatos, G. Wang, A. J. Conejo, and G. B. Giannakis, "Stochastic reactive power management in microgrids with renewables," *IEEE Trans. on Power Systems*, vol. 30, no. 6, pp. 3386–3395, 2015.
- [7] M. Farivar, C. R. Clarke, S. H. Low, and K. M. Chandy, "Inverter var control for distribution systems with renewables," *Proc. of IEEE International Conference on Smart Grid Communications (SmartGridComm)*, pp. 457–462, 2011.
- [8] J. Lavaei and S. H. Low, "Zero duality gap in optimal power flow problem," *IEEE Trans. on Power Systems*, vol. 27, no. 1, pp. 92–107, 2012.
- [9] S. H. Low, "Convex relaxation of optimal power flow—Part I: Formulations and equivalence," *IEEE Trans. on Control of Network Systems*, vol. 1, no. 1, pp. 15–27, 2014.
- [10] —, "Convex relaxation of optimal power flow—Part II: Exactness," *IEEE Trans. on Control of Network Systems*, vol. 1, no. 2, pp. 177–189, 2014.
- [11] V. Kekatos, L. Zhang, G. B. Giannakis, and R. Baldick, "Voltage regulation algorithms for multiphase power distribution grids," *IEEE Trans. on Power Systems*, vol. 31, no. 5, pp. 3913–3923, 2016.
- [12] K. Baker, A. Bernstein, E. Dall'Anese, and C. Zhao, "Network-cognizant voltage droop control for distribution grids," *arXiv preprint arXiv:1702.02969*, 2017.
- [13] E. Dall'Anese, S. V. Dhople, and G. B. Giannakis, "Optimal dispatch of photovoltaic inverters in residential distribution systems," *IEEE Trans. on Sustainable Energy*, vol. 5, no. 2, pp. 487–497, 2014.
- [14] X. Zhou, E. Dall'Anese, L. Chen, and A. Simonetto, "An incentive-based online optimization framework for distribution grids," *IEEE Trans. on Automatic Control*, 2017.
- [15] X. Zhou, E. Dall'Anese, and L. Chen, "Online stochastic control of discrete loads in distribution grids," *arXiv preprint arXiv:1711.09953*, 2017.
- [16] N. Li, G. Qu, and M. Dahleh, "Real-time decentralized voltage control in distribution networks," *Proc. of Annual Allerton Conference on Communication, Control, and Computing (Allerton)*, pp. 582–588, 2014.
- [17] S. Bolognani and S. Zampieri, "A distributed control strategy for reactive power compensation in smart microgrids," *IEEE Trans. on Automatic Control*, vol. 58, no. 11, pp. 2818–2833, 2013.
- [18] S. Magnusson, C. Fischione, and N. Li, "Voltage control using limited communication," *arXiv preprint arXiv:1704.00749*, 2017.
- [19] Q. Peng and S. H. Low, "Distributed optimal power flow algorithm for radial networks, I: Balanced single phase case," *IEEE Trans. on Smart Grid*, 2016.

- [20] P. Šulc, S. Backhaus, and M. Chertkov, "Optimal distributed control of reactive power via the alternating direction method of multipliers," *IEEE Trans. on Energy Conversion*, vol. 29, no. 4, pp. 968–977, 2014.
- [21] W. Shi, X. Xie, C. C. Chu, and R. Gadh, "Distributed optimal energy management in microgrids," *IEEE Trans. on Smart Grid*, vol. 6, no. 3, pp. 1137–1146, 2015.
- [22] S. Magnússon, P. C. Weeraddana, and C. Fischione, "A distributed approach for the optimal power-flow problem based on ADMM and sequential convex approximations," *IEEE Trans. on Control of Network Systems*, vol. 2, no. 3, pp. 238–253, 2015.
- [23] M. Bazrafshan and N. Gatsis, "Decentralized stochastic optimal power flow in radial networks with distributed generation," *IEEE Trans. on Smart Grid*, vol. 8, no. 2, pp. 787–801, 2017.
- [24] C. Wu, G. Hug, and S. Kar, "Distributed voltage regulation in distribution power grids: Utilizing the photovoltaics inverters," *Proc. of American Control Conference (ACC), 2017*, pp. 2725–2731, 2017.
- [25] J. W. Simpson-Porco, F. Dörfler, and F. Bullo, "Voltage stabilization in microgrids via quadratic droop control," *IEEE Trans. on Automatic Control*, vol. 62, no. 3, pp. 1239–1253, 2017.
- [26] H. Zhu and H. J. Liu, "Fast local voltage control under limited reactive power: Optimality and stability analysis," *IEEE Trans. on Power Systems*, vol. 31, no. 5, pp. 3794–3803, 2016.
- [27] X. Zhou, J. Tian, L. Chen, and E. Dall'Anese, "Local voltage control in distribution networks: A game-theoretic perspective," *Proc. of North American Power Symposium (NAPS)*, pp. 1–6, 2016.
- [28] X. Zhou and L. Chen, "An incremental local algorithm for better voltage control in distribution networks," *Proc. of IEEE Conference on Decision and Control (CDC)*, pp. 2396–2402, 2016.
- [29] P. Jahangiri and D. C. Aliprantis, "Distributed Volt/VAR control by PV inverters," *IEEE Trans. on power systems*, vol. 28, no. 3, pp. 3429–3439, 2013.
- [30] B. A. Robbins, C. N. Hadjicostis, and A. D. Domínguez-García, "A two-stage distributed architecture for voltage control in power distribution systems," *IEEE Trans. on Power Systems*, vol. 28, no. 2, pp. 1470–1482, 2013.
- [31] K. Turitsyn, P. Šulc, S. Backhaus, and M. Chertkov, "Options for control of reactive power by distributed photovoltaic generators," *Proc. of the IEEE*, vol. 99, no. 6, pp. 1063–1073, 2011.
- [32] D. K. Molzahn, F. Dörfler, H. Sandberg, S. H. Low, S. Chakrabarti, R. Baldick, and J. Lavaei, "A survey of distributed optimization and control algorithms for electric power systems," *IEEE Trans. on Smart Grid*, 2017.
- [33] F. Andren, B. Bletterie, S. Kadam, P. Kotsampopoulos, and C. Bucher, "On the stability of local voltage control in distribution networks with a high penetration of inverter-based generation," *IEEE Trans. on Industrial Electronics*, vol. 62, no. 4, pp. 2519–2529, 2015.
- [34] B. Zhang, A. D. Dominguez-Garcia, and D. Tse, "A local control approach to voltage regulation in distribution networks," *Proc. of IEEE North American Power Symposium (NAPS), 2013*, pp. 1–6, 2013.
- [35] L. Chen, S. H. Low, and J. C. Doyle, "Random access game and medium access control design," *IEEE/ACM Trans. on Networking (TON)*, vol. 18, no. 4, pp. 1303–1316, 2010.
- [36] F. P. Kelly, A. K. Maulloo, and D. K. Tan, "Rate control for communication networks: shadow prices, proportional fairness and stability," *Journal of the Operational Research society*, vol. 49, no. 3, pp. 237–252, 1998.
- [37] S. H. Low, "A duality model of tcp and queue management algorithms," *IEEE/ACM Trans. On Networking*, vol. 11, no. 4, pp. 525–536, 2003.
- [38] S. H. Low and D. E. Lapsley, "Optimization flow control. i. basic algorithm and convergence," *IEEE/ACM Trans. on networking*, vol. 7, no. 6, pp. 861–874, 1999.
- [39] F. Chandra, D. F. Gayme, L. Chen, and J. C. Doyle, "Robustness, optimization, and architectures," *European Journal of Control*, vol. 17, no. 5-6, pp. 472–482, 2011.
- [40] L. Chen, S. Low, M. Chiang, and J. Doyle, "Cross-layer congestion control, routing and scheduling design in ad hoc wireless networks," *Proc. of IEEE International Conference on Computer Communications (INFOCOM)*, pp. 1–13, 2006.
- [41] M. Chiang, S. H. Low, R. Calderbank, and J. C. Doyle, "Layering as optimization decomposition," *Proc. of IEEE*, vol. 95, no. 1, pp. 255–312, 2007.
- [42] J. Doyle, J. Carlson, S. Low, F. Paganini, G. Vinnicombe, W. Willinger, J. Hickey, P. Parrilo, and L. Vandenberghe, *Robustness and the internet: Theoretical foundations*. Mar. 2002, vol. 5.
- [43] L. Chen and S. You, "Reverse and forward engineering of frequency control in power networks," *IEEE Trans. on Automatic Control*, vol. 62, no. 9, pp. 4631–4638, 2017.
- [44] N. Li, C. Zhao, and L. Chen, "Connecting automatic generation control and economic dispatch from an optimization view," *IEEE Trans. on Control of Network Systems*, vol. 3, no. 3, pp. 254–264, 2016.
- [45] X. Zhou and L. Chen, "A new perspective to synchronization in networks of coupled oscillators: Reverse engineering and convex relaxation," *IFAC-PapersOnLine*, vol. 48, no. 22, pp. 40–45, 2015.
- [46] L. Chen and N. Li, "On the interaction between load balancing and speed scaling," *IEEE Journal on Selected Areas in Communications*, vol. 33, no. 12, pp. 2567–2578, 2015.
- [47] G. Ding and L. Chen, "Load balancing and speed scaling interaction in processor-sharing systems with exponential power functions," *Proc. of Annual Allerton Conference on Communication, Control, and Computing (Allerton)*, pp. 1197–1203, 2016.
- [48] Z. Liu and L. Chen, "Proportional control applied to dynamic network resource allocation," *Proc. of American Control Conference (ACC)*, pp. 1948–1953, 2017.
- [49] M. E. Baran and F. F. Wu, "Network reconfiguration in distribution systems for loss reduction and load balancing," *IEEE Trans. on Power Delivery*, vol. 4, no. 2, pp. 1401–1407, 1989.
- [50] Z. Liu, J. Shihadeh, S. You, G. Ding, X. Zhou, and L. Chen, "Signal-anticipating in local voltage control in distribution systems," *arXiv*, 2018.
- [51] J. Wen, Q. Wu, D. Turner, S. Cheng, and J. Fitch, "Optimal coordinated voltage control for power system voltage stability," *IEEE Trans. on Power Systems*, vol. 19, no. 2, pp. 1115–1122, 2004.
- [52] H. K. Khalil, *Nonlinear Systems*. Englewood Cliffs, NJ: Prentice Hall, 2002.
- [53] R. D. Zimmerman, C. E. Murillo-Sánchez, and R. J. Thomas, "MATPOWER: Steady-state operations, planning, and analysis tools for power systems research and education," *IEEE Trans. on Power Systems*, vol. 26, no. 1, pp. 12–19, 2011.
- [54] M. Farivar, L. Chen, and S. Low, "Equilibrium and dynamics of local voltage control in distribution systems," *Proc. of IEEE Conference on Decision and Control (CDC)*, pp. 4329–4334, 2013.
- [55] M. Farivar, X. Zhou, and L. Chen, "Local voltage control in distribution systems: An incremental control algorithm," *Proc. of IEEE International Conference on Smart Grid Communications (SmartGridComm)*, pp. 732–737, 2015.
- [56] X. Zhou, M. Farivar, and L. Chen, "Pseudo-gradient based local voltage control in distribution networks," *Proc. of IEEE Annual Allerton Conference on Communication, Control, and Computing*, pp. 173–180, 2015.